Deliverable D13.4: Initial report on assimilation activities

Work package no	**WP***13*		
Deliverable no.	**D13.***4*		
Lead beneficiary	**ECMWF**		
Deliverable type	v☐ R (Document, report)		
	☐ DEC (Websites, patent fillings, videos, etc.)		
	☐ OTHER: please specify **..**		
Dissemination level	v☐ PU (public)		
	☐ CO (confidential, only for members of the Consortium, incl Commission)		
Estimated delivery date	**Month** *23*		
Actual delivery date	*28/04/2017*		
Version	**Final**		
Comments			

D13.4: INITIAL REPORT ON ASSIMILATION ACTIVITIES

13.4.1. INTRODUCTION

This report presents examples of the assimilation activities that have been funded in ACTRIS-2 Joint Research Activity 3 (JRA3/WP13) to facilitate data uptake and usage from operational and research centres which engage in aerosol modelling and forecasting activities both at the regional and global scales. The common strategy has been to coordinate with the data centres (NILU, CNR and CNRS) and acquire datasets that are relevant for assimilation according to the specific applications at the various centres. For example BSC has been focusing on assimilation of lidar profiles for improvements in the dust forecast, whereas at RIUUK, initial efforts have been made to look at volcanic ash. ECMWF's activities have been centred on the assimilation of profile information to improve the aerosol description at selected EARLINET/ACTRIS stations with future NRT capabilities as demonstrated during a campaign in 2012 when data where acquires continuously over a period of 72h.

13.4.2 ASSIMILATION ACTIVITIES AT BSC (Enza Di Tomaso, Oriol Jorba and Carlos Pérez García-Pando, BSC, Qiaoyun Hu, Université de Lille)

The vertical structure of dust plumes needs to be better represented in model simulations (Binietoglou et al., 2015). High uncertainties in our representation of dust vertical structure have implications for the radiation's budget and transport. Despite this, model vertical structures are generally poorly constrained by observations. BSC's data assimilation activities aim to tackle the difficulties in constraining dust aerosol information in the vertical, making use of model simulations from the chemical weather prediction system NMMB-MONARCH v1.0, formerly known as NMMB/BSC-Dust (Pérez et al., 2011), enhanced with data assimilation capability.

Data assimilation scheme

NMMB-MONARCH has been coupled with an ensemble-based data assimilation technique known as LETKF (Hunt et al., 2007). For this purpose a forecast ensemble based on known uncertainties in the physical parametrizations of the mineral dust emission scheme has been created. The main developments for the enhancement of the NMMB-MONARCH v1.0 with a data assimilation capability are described in Di Tomaso et al. (2017). Here we will describe additional features that have been added, or are particular relevant, to deal with observational profile information.

The sparse nature of lidar ground-based observations is better handled with reasonably high resolution simulations, which are more efficiently run on a regional, rather than a global, domain. Therefore, the data assimilation scheme, initially built for a global regular grid, has been adapted to the NMMB-MONARCH regional rotated coordinate system. The rotated frame is used in order to reduce the variation of the grid size.

Subsequently, the observation operator H has been built for ground-based extinction profiles at 532 nm. H consists in calculating the model equivalent of the observations, i.e. to map the ensemble mean state vector into the observation space. Hence it has two components: vertical and horizontal interpolation component, followed by the calculation of an extinction profile from a model mass concentration profile.

The observation vertical information is interpolated at the mid altitude of the model layers using a third-order polynomial interpolation function. Model tracers are then interpolated at the observation location at each model level. The simulated extinction for wavelength λ is calculated at a given observation location according to the following linear operator:

$$\text{ext}_\lambda = \sum \frac{3 \text{qext}_{b\lambda} c_b}{4 r_b \rho_b} \qquad (1)$$

where ρ_b [kg m−3] is the particle mass density, rb [m] is the effective radius, cb [kg m−3] is the dust mass concentration for each dust bin, and qext_λ is the extinction efficiency factor. The extinction efficiency factors for 532 nm have been calculated using the Mie scattering theory (Mishchenko et al., 2002) assuming dust spherical, non-soluble particles for the 8 model size bins, and, within a bin, a lognormal distribution for dust with geometric radius of 0.2986 μm and standard deviation of 2.0, and using information on refractive indices at different wavelength from the OPAC database (Hess et al., 1998). The imaginary part of the refractive index has been interpolated from the available values at 500 and 550 nm. Extinction efficiency factors for NMMB-MONARCH v1.0 8 bins are estimated as 1.489289, 3.438292, 3.109589, 2.458298, 2.251090, 2.253891, 2.149677, 2.1017. In our future work we plan to revise our choice of optical properties since the OPAC database is known to provide a too absorptive dust aerosol (Kaufman et al., 2001). Since we use in the state vector the total mass mixing ratio, an ensemble averaged extinction efficiency is calculated during the assimilation as in Schutgens et al. (2010) as an average of the extinction efficiency of the individual bins weighted by the bin mixing ratios.

We use a 24-hour assimilation window and observations are considered for assimilation at four time slots within the window, at 0, 6, 12 and 18 UTC. The system uses as first guess a 1-day forecast with output every 6 hours. Simulated observation and background departures are calculated at each time slot. We are using the LETKF implementation with a four-dimensional extension as described in Hunt et al. (2007). The state vector comprises of the mixing ratio at all the time slots considered. Background observation means and perturbation matrices are formed at the various time slots when the observations are available. They are then vertically concatenated to form a combined background observation mean and perturbation matrix which are used for the standard LETKF calculations, i.e. the analysis increments are based on all innovations throughout the day.

Vertical and horizontal localization are performed through R-localization, i.e. the localization is performed in the observation error covariance matrix, making the influence of an observation on the analysis decay gradually toward zero as the distance from the analysis location increases. To achieve this, the observation error is divided by a distance dependent function that decays to zero with increasing distance: $e^{\frac{-\text{dist}^2}{l^2}}$, where dist is the distance in the grid space between an observation and the model grid in which the analysis is calculated, and l is horizontal or vertical localisation factor. We apply both horizontal and vertical localization, and use a horizontal localization factor equal to 2. This means that observation's influence in the horizontal plane will become negligible at distances greater than 3 to 4 grid points (the actual distance is resolution dependent).

Observational data

Profile observations were provided by the University of Lille for the M'bour site outside Dakar, in Senegal, for case studies of dust intrusions observed with a multi-wavelength Mie-Raman lidar

(Bovchaliuk et al., 2016, and Veselovskii et al., 2016). The spectral extinction profiles are provided at two wavelength: 355 nm, and 532 nm for a profile of range of signal. However, we have assimilated only profiles at 532 nm. Observation height h is calculated from the range s of the signal with h=s*cos(46.5°). All the extinction profiles are computed by averaging 2-hour lidar signals except when some of the measurements are not available. All the night time extinction profiles are derived from the Raman method, while the daytime extinction profiles are calculated from the Klett method. The assumed lidar ratio that is required for the Klett method is taken from the nearest night time Raman retrieval. Due the overlap range of the lidar system, only signal above 700 m (in height) is considered valid. For this reason, only observations above 700 m are used for data assimilation.

Data assimilation experiments

We have run a lidar assimilation experiment for the dust event occurring on March 30-31 2015 in the Dakar region. The simulation domain is the one shown in Figure 1. Simulations were run with 40 hybrid pressure-σ layers, and a horizontal resolution of 0.33° by 0.33°. We have assimilated observations from model level 7 to 17, i.e. above 700 m and up to 4000 m circa. LETKF has the advantageous feature that it applies localization, i.e. it performs the analysis locally. At each grid point only observations within a 4 grid point distance (i.e. 1.3° circa) were assimilated. No inflation of the ensemble spread has been used.

We have run a free ensemble simulation, without assimilating any observation, starting in mid-February 2015 from a deterministic control experiment, to spin-up the ensemble before data assimilation. The spin-up period for the ensemble ensures that perturbations applied at the sources propagate everywhere.

Figure 1 shows the dust AOD analysis at 550 nm at three time steps of the assimilation window. The corresponding analysis increments are shown in Figure 2. For this particular event the assimilated profile corrects an underestimation in total column extinction in the model. Though observations were available only at 18 UTC, the 4D extension used for the LETKF propagates the observational impact through the whole assimilation window.
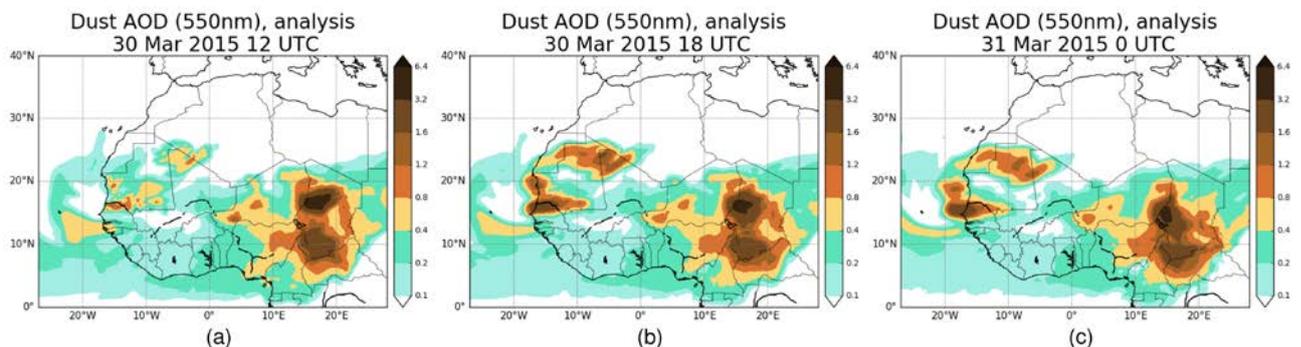
Figure1: Dust AOD analysis at 550 nm at three time steps of the assimilation window produced by the assimilation of a lidar extinction profile at the M'Bour site in Senegal. The profile was measured on 30 March 2015 at 18 UTC.
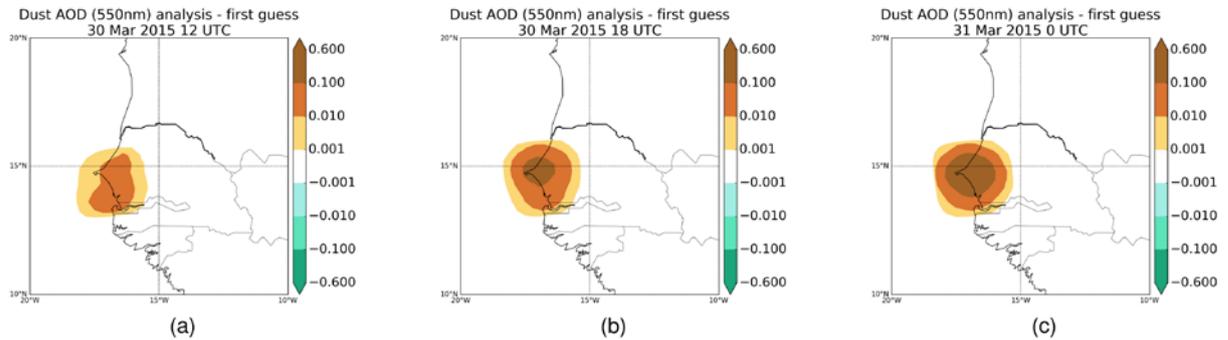
Figure 2: Analysis increments (analysis – first guess) corresponding to the three analyses of Figure 1.

Figure 3 shows the extinction profiles at 532 nm at the lidar site location for the model first guess, the analysis, and, when available, for the observations at three time steps of the assimilation window. These results refer to having used an observation uncertainty described by the diagonal observation error covariance matrix with elements equal to 0.0001+0.01*ext532, and a vertical localization factor set to the value 1. Such a setting means that after two grid points the influence of an observation is negligible. As a sanity check we can note that the analysis is closer to the assimilated observations than the first guess (Figure 3b).
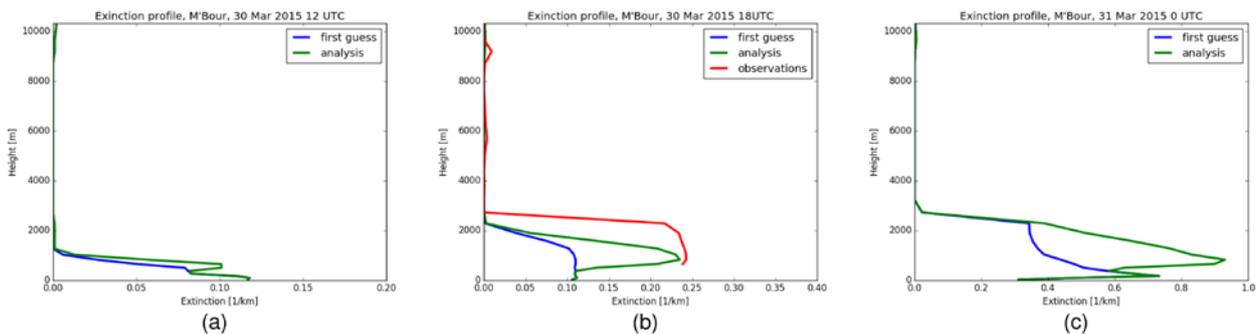

Figure 3: Extinction profiles at 532 nm for the model first guess (blue), the analysis (green), and, when available, for the assimilated observations (red) at the M'Bour site at three time steps of the assimilation window.

When a higher observation uncertainty is used (0.0001+0.1* ext532), there are only minor analysis corrections (Figure 4a). This might be due to an under-representation of the background uncertainty which translated into giving a lower weight to the observations with respect to the background. Background error statistics in our system should be investigated further in order to assess how well our ensemble configuration represents model uncertainty.

Increasing the vertical localization factor to the value 2 produces an overestimation of profile peak in the analysis (Figure 4b). Further work should go into identifying a better function for the vertical localization than the one we have used. While in the horizontal grid of reference distances between grid points can be used, with some approximation, as a proxy for real distances, in the vertical grid of reference this approximation is less correct. In our future work we plan to test the calculation of vertical distances in physical space rather than in grid space.
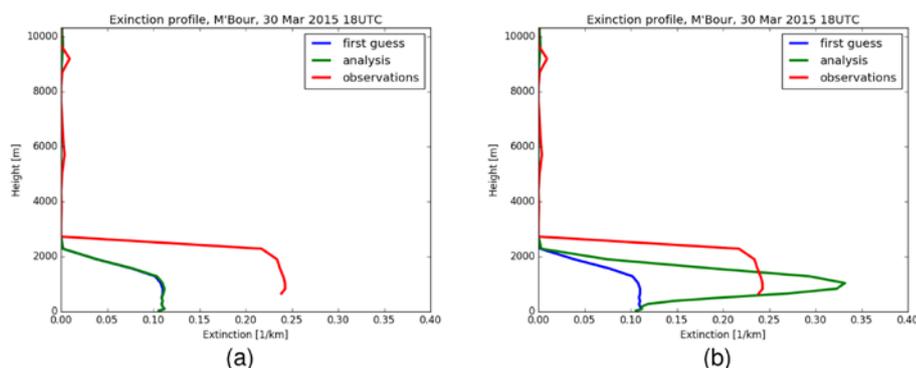
Figure 4: As the central panel of Figure 3, but for a different observation uncertainty characterization (a), and a different vertical localization factor (b).

References

Binietoglou, I., S. Basart, L. Alados-Arboledas, V. Amiridis, ...U. Wandinger, and J. Wagner: A methodology for investigating dust model performance using synergistic EARLINET/AERONET dust concentration retrievals, Atmos. Meas. Tech., 8, 3577-3600, doi:10.5194/amt-8-3577-2015, 2015.

Bovchaliuk, V., Goloub, P., Podvin, T., Veselovskii, I., Tanre, D., Chaikovsky, A., Dubovik, O., Mortier, A., Lopatin, A., Korenskiy, M., and Victori, S.: Comparison of aerosol properties retrieved using GARRLiC, LIRIC, and Raman algorithms applied to multi-wavelength lidar and sun/sky-photometer data, Atmos. Meas. Tech., 9, 3391-3405, doi:10.5194/amt-9-3391-2016, 2016.

Di Tomaso, E., Schutgens, N. A. J., Jorba, O., and Pérez García-Pando, C.: Assimilation of MODIS Dark Target and Deep Blue observations in the dust aerosol component of NMMB-MONARCH version 1.0, Geosci. Model Dev., 10, 1107-1129, doi:10.5194/gmd-10-1107-2017, 2017.

Hess, M., P. Koepke, and I. Schult: Optical Properties of Aerosols and Clouds: The software package OPAC, Bull. Am. Met. Soc., 79, 831-844, 1998.

Hunt, B. R., Kostelich, E. J., and Szunyogh, I.: Efficient data assimilation for spatiotemporal chaos: A local ensemble transform Kalman filter, Physica D, 230, 112–126, 2007.

Kaufman, Y. J ., D. Tanré, O. Dubovik, A. Karnieli, and L. A. Remer: Absorption of sunlight by dust as inferred from satellite and ground-based remote sensing, Geophys. Res. Lett., 28, 1479–1482, 2001.

Mishchenko, M. I., L. D. Travis, and A. A. Lacis: Scattering, Absorption, and Emission of Light by Small Particles. Cambridge University Press, Cambridge, 2002.

Pérez, C., Haustein, K., Janjic, Z., Jorba, O., Huneeus, N., Baldasano, J. M., Black, T., Basart, S., Nickovic, S., Miller, R. L., Perlwitz, J. P., Schulz, M., and Thomson, M.: Atmospheric dust modeling from meso to global scales with the online NMMB/BSC-Dust model – Part 1: Model description, annual

simulations and evaluation, Atmos. Chem. Phys., 11, 13001–13027, doi:10.5194/acp-11-13001-2011, 2011.

Schutgens, N. A. J., Miyoshi, T., Takemura, T., and Nakajima, T.: Sensitivity tests for an ensemble Kalman filter for aerosol assimilation, Atmos. Chem. Phys., 10, 6583–6600, doi:10.5194/acp-10-6583-2010, 2010.

Veselovskii, I., Goloub, P., Podvin, T., Bovchaliuk, V., Derimian, Y., Augustin, P., Fourmentin, M., Tanre, D., Korenskiy, M., Whiteman, D. N., Diallo, A., Ndiaye, T., Kolgotin, A., and Dubovik, O.: Retrieval of optical and physical properties of African dust from multiwavelength Raman lidar measurements during the SHADOW campaign in Senegal, Atmos. Chem. Phys., 16, 7013-7028, doi:10.5194/acp-16-7013-2016, 2016.

13.4.3. ASSIMILATION ACTIVITIES AT ECMWF (JULIE LETERTRE-DANCZAK AND ANGELA BENEDETTI, ECMWF, LUCIA MONA, CNR)

The assimilation of lidar data as the backscatter or extinction coefficient is a new challenge for the ECMWF aerosol analysis. These parameters will give access to a better understanding of the aerosol vertical distribution and a better aerosol forecast from the model.

Since 2015, studies have been started at ECMWF to evaluate the impact of lidar data on the ECMWF system in the so-called C-IFS configuration (Composition in Integrated Forecast System). The first data assimilated were the CALIOP level 1.5. This product consists attenuated backscatter at 532nm, cloud-cleared and average at a horizontal resolution of 20km. This product was created explicitly for assimilation purposes, courtesy of Dr Winker and his team at NASA Langley. The latest model version used was cycle 40R2. Assimilation of this data was very encouraging and promising on the vertical distribution but a bias on the AOD appeared in comparison with AERONET (which was not the case for the assimilation of only MODIS data). This could be due to several reasons both related to model and observations biases, but as a consequence the operational assimilation of CALIOP was postponed. Further details are provided in Benedetti and Dabas, 2016.

At the moment ECMWF runs two projects related to lidar assimilation: one on the assimilation of EarthCARE and Aeolus lidar data (A3S) and the other on the assimilation of ground based lidar which is part of the ECMWF's contribution to ACTRIS-2. In this report the first steps in the assimilation of the ground-based lidars will be outlined.

The process of assimilation has started at ECMWF using a set of data from EARLINET corresponding to a campaign of 72h in July 2012 (Sicard et al 2015, D'Amico et al 2015). The location of the different lidars used during this campaign can be seen on Figure 5. A new code in python was developed to convert the data from NETCDF to ODB, which is the standard format file used inside the ECMWF assimilation code. Because the structure of the code is strictly defined, we had to make some average on the data to have a consistent number of vertical layer between stations and at different times. The number of fixed layers chosen is 67 with a vertical resolution of 250m. All profiles measured on a period

of 12 hours are grouped in one file. If the maximum altitude of the profile is reached before the maximum authorized, a constant value is set up at -2147483647 corresponding to a missing value in the ODB file.

Figure 5. Geographical position of the 11 stations EARLINET. Green labels indicate advanced lidar systems; orange labels indicate Raman lidar systems. Yellow circles indicate co-located sun photometers.

Once the files were generated, the observation operator for the assimilation of lidar parameters was upgraded. This code was already existing for CALIOP data, but the difference in the origin of the measurement (ground or space) and the definition of the backscatter (attenuated or aerosol) had to be defined and extended. For the moment, the system is able to ingest one parameter (backscatter or extinction) for one wavelength for one instrument, which mean we are unable to make any cross assimilation of data at different wavelengths. This capability will be developed in the next few months. Moreover, the possibility of assimilating simultaneously both ground-based and satellite lidar data will also be developed. This will allow to use the ground-based lidar data as anchor for the bias correction of the satellite (CALIOP) data.

The first assimilation of the EARLINET data gave interesting, if preliminary, results (see *Figure 6*6). First of all, it can be noticed that the background backscatter coefficient is always very low (close to zero). The observations assimilated (red in the bottom plot) are between altitude 5 and 10 km, while under 5km the observations seem to be rejected systematically (blue in the bottom plot). Regardless the fact that only a fraction of the data are effectively assimilated, there is an impact on the analysis departures (differences between analysis and background). More investigation is currently under way.
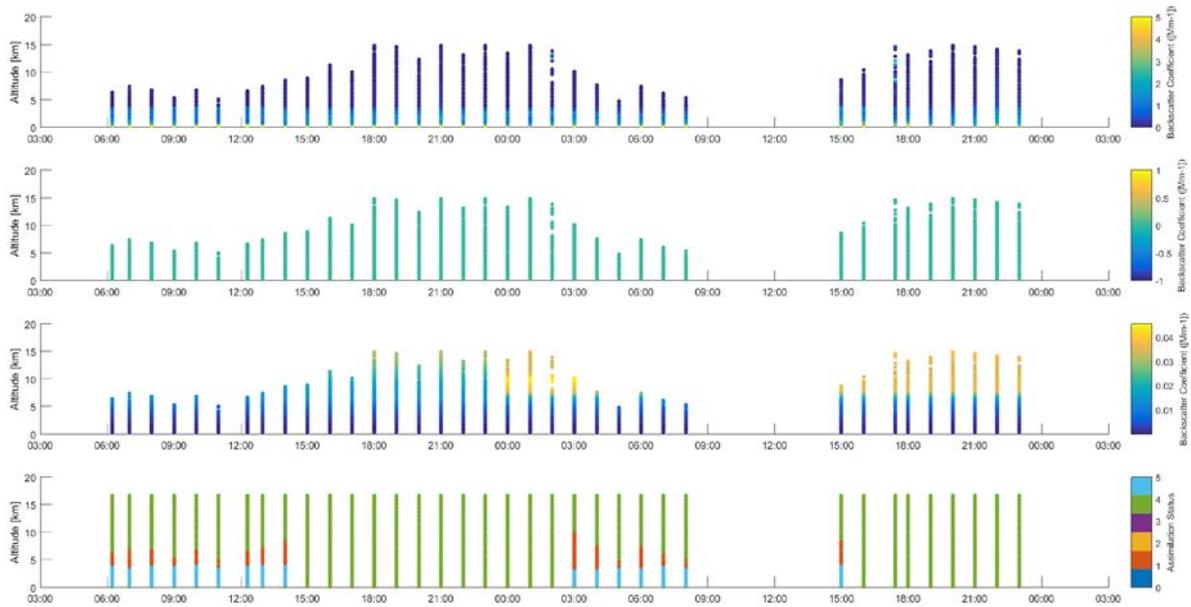
Figure 6. Impact of assimilation of aerosol backscatter coefficient at 532nm for the 09th and 10th July 2012 at Barcelona (Spain), from top to bottom: observation, background, analysis, status of observation in the assimilation.

In the meantime, in the framework of TOPROF, Maxime Hervo from MeteoSwiss visited ECMWF for two weeks to try the assimilation of ceilometer data, using recent observations (March 2017). This work is still in progress and will be done in parallel with the ACTRIS-2 work to maximize synergies. Figure 7 shows the spatial distribution in Europe of the ceilometer network.
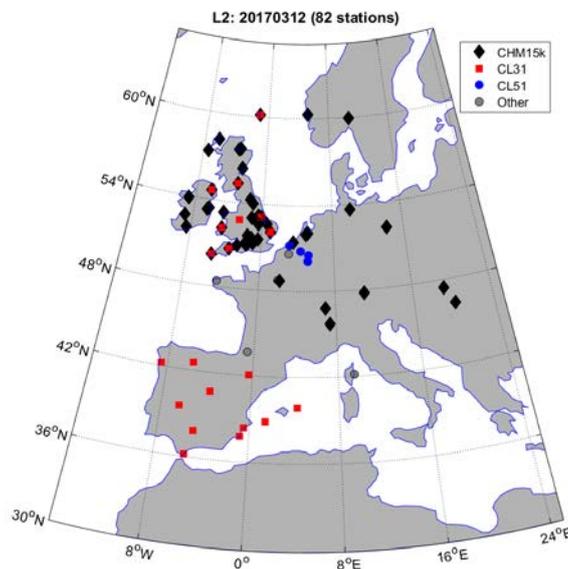

Figure 7. Geographical location of 82 stations ceilometer E-PROFILE, black diamonds: CHM15k, red squares: CL31, blue squares: CL51 and grey circle MPL lidars. (Courtesy M. Hervo).

References

Benedetti, A. and A. Dabas (2016), "Assessment of the necessary developments to assimilate Aeolus and EarthCARE aerosol profile products", Technical Note 1 of ESA contract number 4000116106. Available from ESA.

Sicard, M. et al.: EARLINET: potential operationality of a research network, Atmos. Meas. Tech., 8, 4587-4613, doi:10.5194/amt-8-4587-2015, 2015.
D'Amico, G. et al.: EARLINET Single Calculus Chain - overview on methodology and strategy, Atmos. Meas. Tech., 8, 4891-4916, doi:10.5194/amt-8-4891-2015, 2015.

13.4.4 ASSIMILATION ACTIVITIES AT RIUUK (ANNE CAROLINE LANGE AND HENDRIK ELBERN)

Objectives

Within work package 13 'Model evaluation, assimilation and trend studies', the Rhenish Institute for Environmental Research at the University of Cologne (RIUUK) works on the application of ACTRIS-2 data for European scale data assimilation. The information content of ACTRIS-2 profiling observations will be quantitatively evaluated.

The focus lies on the assessment of aerosol source strength estimations of volcanic eruptions and specifically on the reanalysis of ash dispersion across Europe during the Eyjafjallajökull eruption in April and May 2010. Likewise, mineral dust loads and transport from the Sahara desert towards Europe will be analysed. Therefore, in addition to ground based ACTRIS-2/EARLINET lidar backscatter profiles, satellite remote sensing data from Meteosat's SEVIRI and Calipso's CALIOP instruments are used as observational data. Realising four-dimensional variational (4d-var) data assimilation in combination with ensemble modelling forecast errors and analysis uncertainties should be estimated, which is of special interest in case of the investigation of air traffic related threshold values after a volcanic eruption.

Methods

For all studies performed by RIUUK, the European Air Pollution Dispersion Inverse Model EURAD-IM is applied. This Eulerian model comprises a chemistry transport model (CTM) including aerosol dynamics and for inverse modelling a 4D-var assimilation system including the adjoint of the reactive chemistry. The special idea of joint emission rate and initial value optimisation by 4D-var is to minimise the scalar cost function J that measures the distance between

- the CTM model run and an appropriate background field
- the CTM model run and the observations

within a predefined assimilation interval $[t_0, t_F]$:

$$J(\delta\mathrm{x}(t_0), \delta\mathrm{e}) = \frac{1}{2}\big(\delta\mathrm{x}(t_0)\big)^T \mathrm{B}^{-1}\delta\mathrm{x}(t_0) + \frac{1}{2}\int_{t_0}^{t_F}(\delta\mathrm{e})^T \mathrm{K}^{-1}\delta\mathrm{e}\ dt$$

$$+ \frac{1}{2}\int_{t_0}^{t_F}\big(\mathrm{d}(t) - \mathrm{H}(t)\delta\mathrm{x}(t)\big)^T \mathrm{R}^{-1}\big(\mathrm{d}(t) - \mathrm{H}(t)\delta\mathrm{x}(t)\big)dt.$$

Here, $\delta\mathrm{x}(t) = \mathrm{x}(t) - \mathrm{x}_b(t)$ and $\delta\mathrm{e}(t) = \mathrm{e}(t) - \mathrm{e}_b(t)$ describe the differences between the background state $\mathrm{x}_b(t)$ and the emissions $\mathrm{e}_b(t)$. $\mathrm{d}(t) := y(t) - H(t)x_b(t)$ is the discrepancy of the observation vector $y(t)$ and the model equivalent to each observation, which is calculated by the observation operator $\mathrm{H}(t)$. The error covariance matrices B,K,R weigh the contribution of the different considered information according to the accuracy of the background values, the emission factors, and the observations, respectively.

To minimise the cost function, the gradient of J with respect to $\delta\mathrm{x}(t_0)$ and $\delta\mathrm{e}$ has to be determined. The adjoint model operator formally integrates from time t_F backward in time to the initial time t_0. Hence applying the LBFGS minimisation, the optimisation procedure provides an optimised initial value and emission factor, which result in the model trajectory of the optimal state analysis.

Running the model in ensemble mode will provide information about the forecast probability. In the scope of observability, the information gain of once observed quantities can be determined by the analysis error covariance matrix $\mathrm{A} = \dfrac{\mathrm{I} - \mathrm{KH})\ \mathrm{B}}{}$, where I is the identity matrix and K describes the Kalman gain matrix.

Results

Skillful forecasts of extreme aerosol events, such as high concentrated ash emitted during a volcanic eruption, are essential for human health and to prevent exposures of aircraft with possibly catastrophic outcome. Numerical chemistry and aerosol transport models need manual adjustments to capture volcanic emissions, but suffer from unknown source emission parameters. Data assimilation is able to correct the analysis with the help of observational knowledge, even if the ash cloud is observed in large distance to the emission source.

Preliminary results on satellite assimilation will be reported here. Investigations on the analysis of the volcanic ash dispersion over Europe during the 2010 Eyjafjallajökull eruption are performed with observational data from Meteosat's Spinning Enhanced Visible and Infrared Imager (SEVIRI). Using the reverse absorption effect, the presence of volcanic ash within the atmosphere is identified and the amount of ash within the column of each detected satellite pixel is derived. These volcanic ash column mass loading measurements are integrated in the EURAD-IM 4D-var system with a suitable observation operator, which is newly developed and implemented together with its adjoint.
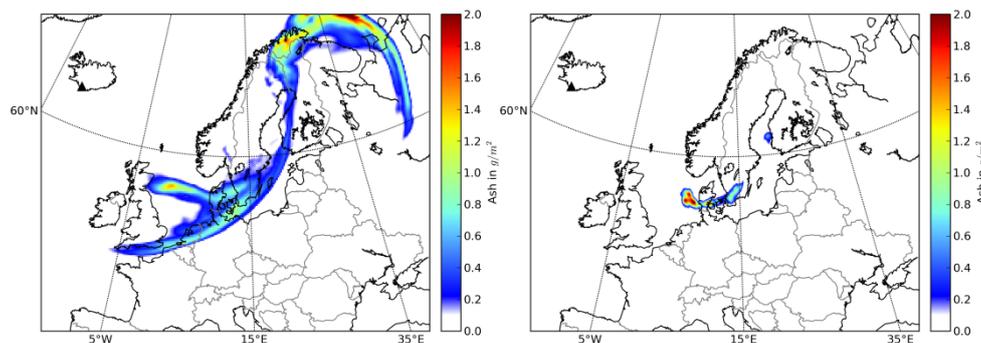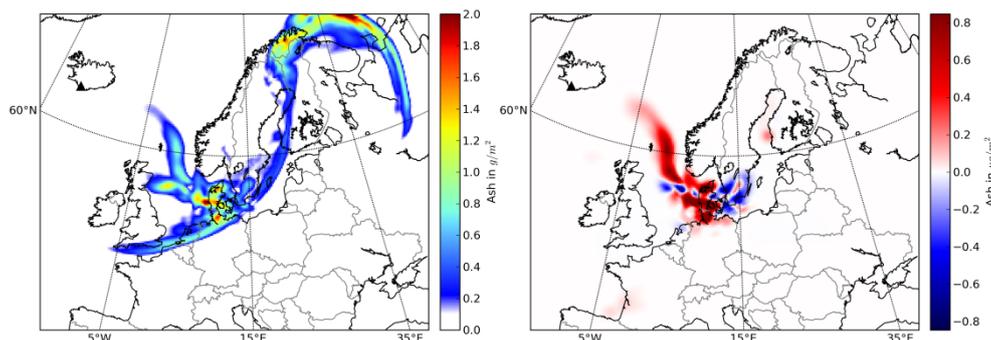
Figure 8: EURAD-IM background simulation (upper-left), cloud limited SEVIRI observations (upper-right), 4D-var analysis (lower-left), and analysis minus background plot (lower-right) of the Eyjafjallajökull volcanic ash distribution over Europe on 16 April 2010, 00:00 UTC.

Assimilation runs are performed mainly for the starting period of the Eyjafjallajökull eruption in April 2010. The focus lies on the optimisation of initial values. The background state is calculated for the period between 14 and 20 April 2010 using volcanic emission profiles according to the plume heights of the weather radar observations in Keflavik and the mass eruption rates derived thereof.

Here, we present the results of the ash distribution over Europe on 16 April 2010, assimilating SEVIRI observations within the assimilation window between 00:00 UTC and 12:00 UTC. In its upper-left panel, *Figure* 8 shows the EURAD-IM background simulation at 00:00 UTC as vertically integrated mass columns. The ash cloud reaches from southern England over the North Sea to Denmark and southern Sweden, to Finland, the North Cape and north-west Russia. At 00:00 UTC the SEVIRI satellite instrument identifies ash only within the region extending from west of Denmark along the south coast of Sweden and another small cloud over south-west coast of Finland (upper-left panel of *Figure* 8). The analysis in the lower-right panel of *Figure* 8 shows increasing ash concentrations in the areas of the observations, especially over Denmark and over the North Sea west of Denmark. The difference plot of analysis minus background (lower-right panel of *Figure* 8) confirms this correction and shows a decrease of ash within the analysis at the peripheral regions of the observations. The increase of ash between the south-west of Norway and Scotland results from corrections induced by observations later in the assimilation window. The missing corrections of simulated ash in the north of Scandinavia are expected due to the geometrical observation limits of the geostationary instrument.

To validate the assimilation performance using SEVIRI data, a comparison with independent observation is accomplished: vertically resolved total attenuated backscatter profiles from CALIOP (Cloud-Aerosol LIdar with Orthogonal Polarisation) are chosen for the comparison with the vertical ash cloud structure of the data assimilation analysis. *Figure* 9 shows in the left panel the CALIPSO profiles over south-west Finland and the Baltic Sea on 16 April 2010 between 01:18 UTC and 01:25 UTC. Volcanic ash is observed between 4.5 km and 6.0 km height from 58.12 °N to 62.43 °N. The centre and right panel of *Figure* 8 depict the vertical cross section along the CALIPSO satellite path of the EURAD-IM ash concentration for the background simulations and the analysis, respectively. Only small differences between background and the analysis can be seen, because only a small SEVIRI detected ash cloud over south-west Finland overlaps with the satellite path of CALIPSO. Due to the adjoint observation operator that redistributes the ash according to the vertical distribution of the background field, the analysis does not present corrections in altitudes of no background ash. But especially between grid cell 20 and grid cell 40, which correspond to the area where CALIPSO identifies ash, stronger

corrections can be seen in the analysis. Generally, fine structures of the vertical ash distribution as detected by CALIOP cannot be represented by the model, due to its coarse vertical grid in the upper troposphere.
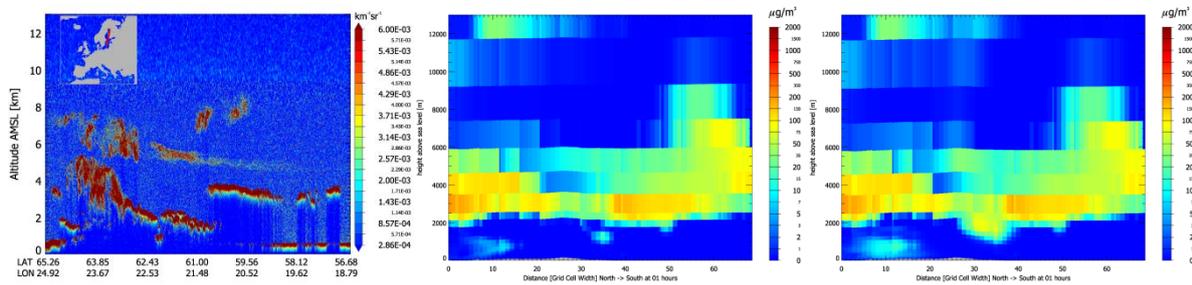

Figure 9: CALIOP attenuated backscatter profiles (left), vertical cross section of EURAD-IM background ash concentration (centre), and vertical cross section of the 4D-var analysis (right) along the CALIPSO satellite path shown in the map inlay on 16 April 2010 at 01:18 UTC to 01:25 UTC.

Subsequently, RIUUK will now focus on the implementations and investigations for the assimilation of lidar observations. The knowledge of the vertical structure of volcanic ash seems very valuable to correct overestimated emissions. Therefore, we will extend the assimilation from initial value optimisation also to emission rate optimisation. The use of ACTRIS-2/EARLINET observations for the assimilation will overcome the unfavourable lack of satellite observations caused by limited transits and cloud occultation.